Chinese Chemical Letters 32 (2021) 2828–2832

Contents lists available at ScienceDirect

Chinese Chemical Letters

journal homepage: www.elsevier.com/locate/cclet

Communication

Combustion synthesis of mesoporous $CoAl_2O_4$ for peroxymonosulfate activation to degrade organic pollutants

Sheng Guo[a,b,c,*], Huiling Tang[a,d], Liming You[b], Huali Zhang[a], Jun Li[e], Kun Zhou[b,c,**]

[a] School of Chemistry and Environmental Engineering, Wuhan Institute of Technology, Wuhan 430205, China
[b] Environmental Process Modelling Centre, Nanyang Environment and Water Research Institute, Nanyang Technological University, Singapore 637141, Singapore
[c] School of Mechanical and Aerospace Engineering, Nanyang Technological University, Singapore 639798, Singapore
[d] Department of Environmental Science and Engineering, Wuhan University, Wuhan 430079, China
[e] Henan Institute of Advanced Technology, Zhengzhou University, Zhengzhou 450052, China

ARTICLE INFO

Article history:
Received 21 October 2020
Received in revised form 7 December 2020
Accepted 12 January 2021
Available online 16 January 2021

Keywords:
$CoAl_2O_4$
Combustion synthesis
Peroxymonosulfate
Sulfate radical
Advanced oxidation process

ABSTRACT

A mesoporous cobalt aluminate ($CoAl_2O_4$) spinel is synthesized through a combustion method and adopted for the activation of peroxymonosulfate (PMS) to degrade organic pollutants. Multiple characterization procedures are conducted to investigate the morphology and physicochemical properties of the $CoAl_2O_4$ spinel. Due to its mesoporous structure, large surface area, and high electrical conductivity, the obtained $CoAl_2O_4$ exhibits remarkable catalytic activity for Rhodamine B (RhB) degradation. Its RhB degradation rate is 89.0 and 10.5 times greater than those of Co_3O_4 and $CoAl_2O_4$ spinel prepared by a precipitation method, respectively. Moreover, the mesoporous $CoAl_2O_4$ spinel demonstrates a broad operating pH range and excellent recyclability. The influence of several parameters (catalyst amount, PMS concentration, initial pH, and coexisting inorganic anions) on the oxidation of RhB is evaluated. Through quenching tests and electron paramagnetic resonance experiments, sulfate radicals are identified as the predominant reactive species in RhB degradation. This paper provides new insights for the development of efficient, stable, and reusable cobalt-based heterogeneous catalysts and promotes the application of persulfate activation technology for the treatment of refractory organic wastewater.

The increasing activities of textile, printing, dyeing, and pharmaceutical industries have led to the discharge of large quantities of wastewater into the aquatic environment [1–3]. Such wastewater is highly stable, contains high concentrations of organic pollutants, and is highly non-biodegradable. It also possesses characteristics of high teratogenicity, carcinogenicity, and biotoxicity, which are greatly detrimental to human health and local ecosystems [4,5]. However, existing water treatment strategies, including physical, chemical, and biological methods, exhibit drawbacks and limitations such as (1) merely changing the phases of pollutants instead of completely degrading them (*e.g.*, adsorption), (2) exhibiting a high operating cost and low degradation efficiency (*e.g.*, chemical oxidation), and (3) demonstrating a general ineffectiveness in degrading toxic and non-biodegradable pollutants (*e.g.*, biological oxidation) [6]. Therefore, developing novel, cost-effective, and efficient technologies for wastewater treatment is a vital imperative.

Recently, an emerging advanced oxidation process (AOP) pertaining to sulfate radicals ($SO_4^{\bullet-}$) has attracted extensive interest in the field of environmental remediation owing to its low cost, high efficiency, and wide application range [7–9]. $SO_4^{\bullet-}$ possesses a higher redox potential ($E^0 = 2.5–3.1$ V) and a longer half-life (30−40 μs) than hydroxyl radicals ($^{\bullet}OH$) produced in Fenton processes, and it is also capable of significantly mineralizing organic pollutants [10]. $SO_4^{\bullet-}$ can be generated by peroxymonosulfate (PMS) and persulfate (PDS) with the incorporation of alkalines, heat, light, ultrasound, carbon materials, and transition metal ions [11–13]. Compared with PDS, PMS exhibits an asymmetric structure and a longer superoxide O—O bond, which increases its probability of being activated [14]. Cobalt ions (Co^{2+}) have proved to be the most effective candidate for activating PMS. However, they are difficult to recover and can potentially result in

* Corresponding author at: School of Chemistry and Environmental Engineering, Wuhan Institute of Technology, Wuhan 430205, China.
** Corresponding author at: Environmental Process Modelling Centre, Nanyang Environment and Water Research Institute, Nanyang Technological University, Singapore 637141, Singapore.
E-mail addresses: guoshengwit@163.com (S. Guo), kzhou@ntu.edu.sg (K. Zhou).

https://doi.org/10.1016/j.cclet.2021.01.019
1001-8417/

secondary pollution [15]. Thus, it is of paramount importance to develop efficient and reusable cobalt-based heterogeneous catalysts for PMS activation.

Spinel-type oxides have received much attention from researchers due to the synergy between their constituent metal atoms, excellent chemical and thermal stability, and high mechanical resistance [16]. The cobalt aluminate ($CoAl_2O_4$) spinel, known as Thenard's blue, is extensively employed as a color filter, pigment layer, as well as an adsorbent and a catalyst for pollutant removal due to its acid-base resistance, excellent chemical stability, good optical properties, and high heat resistance [17–19]. Some spinel-type oxides, such as $CoFe_2O_4$ [20], $CuCo_2O_4$ [21], and $NiCo_2O_4$ [22], have demonstrated high efficiency in activating PMS for pollutant degradation. Thus, it is postulated that $CoAl_2O_4$ can also function as a PMS activator for the treatment of organic pollutants.

Herein, mesoporous $CoAl_2O_4$ with a spinel structure was synthesized by a combustion method, and it was used for the degradation of organic contaminants through PMS activation for the first time. The effects of catalyst loading, PMS dosage, initial pH, and common ions on the catalytic performance were evaluated systematically. Meanwhile, the stability and general applicability of the catalyst were also investigated, and the dominant active species and degradation mechanism in the catalytic degradation system were analyzed.

Analytical reagent-grade chemicals of cobalt nitrate hexahydrate, aluminum nitrate nonahydrate, and triethanolamine were obtained from Sinopharm Chemical Co., Ltd. All the other chemical reagents were of analytical grade. $CoAl_2O_4$ was prepared through a combustion method based on existing literature [23]. First, 10 mmol/L of cobalt nitrate and 20 mmol/L of aluminum nitrate were added to 30 mL of deionized water, respectively. Then, the two solutions were added to a beaker and stirred for 30 min. Afterwards, 12 mL of triethanolamine was introduced to the solution as a fuel with a 2:1 molar ratio of triethanolamine to the total metal ions. A rose-colored flocculent precipitate was then formed, and HCl (12 mol/L) was added dropwise to the mixture until a clear rose-colored solution was obtained. The solution was further heated at 100 °C to remove excess water. Finally, the obtained product was converted to mesoporous $CoAl_2O_4$ by thermal decomposition at 500 °C for 3 h. Co_3O_4 was prepared by a similar procedure, in which aluminum nitrate was not added.

For comparison, a $CoAl_2O_4$ sample was also synthesized by a precipitation-calcination method. Briefly, 20 mmol/L of aluminum nitrate was added dropwise to 10 mmol/L of cobalt nitrate solution under magnetic stirring. Afterwards, the solution pH was adjusted to 10 by adding NaOH. The precipitate was washed with deionized water and heated at 100 °C for 2 h. Finally, the residue was calcinated at 500 °C for 3 h and designated as $CoAl_2O_4$-p. The characterization details of the catalysts and the experimental procedures are provided in Supporting information.

Figs. 1a and b reveal the typical scanning electron microscopy (SEM) images of Co_3O_4 and $CoAl_2O_4$. Co_3O_4 exhibits an octahedral morphology in high yield. The average particle size was measured to be approximately 2 μm. As for $CoAl_2O_4$, such an octahedral morphology was partly destroyed due to the Al atoms occupying the octahedral coordination sites.

The crystal structures of $CoAl_2O_4$ and Co_3O_4 were characterized by X-ray diffraction (XRD), as illustrated in Fig. 1c. The XRD peaks of $CoAl_2O_4$ and Co_3O_4 are identical to those of the cubic spinel phase of $CoAl_2O_4$ (JCPDS No. 44-0160) and Co_3O_4 (JCPDS No. 42-1467), respectively [24]. The positions of the XRD peaks are almost identical since $CoAl_2O_4$ and Co_3O_4 share the same spinel cubic (Fd3m) crystallographic structure [25].

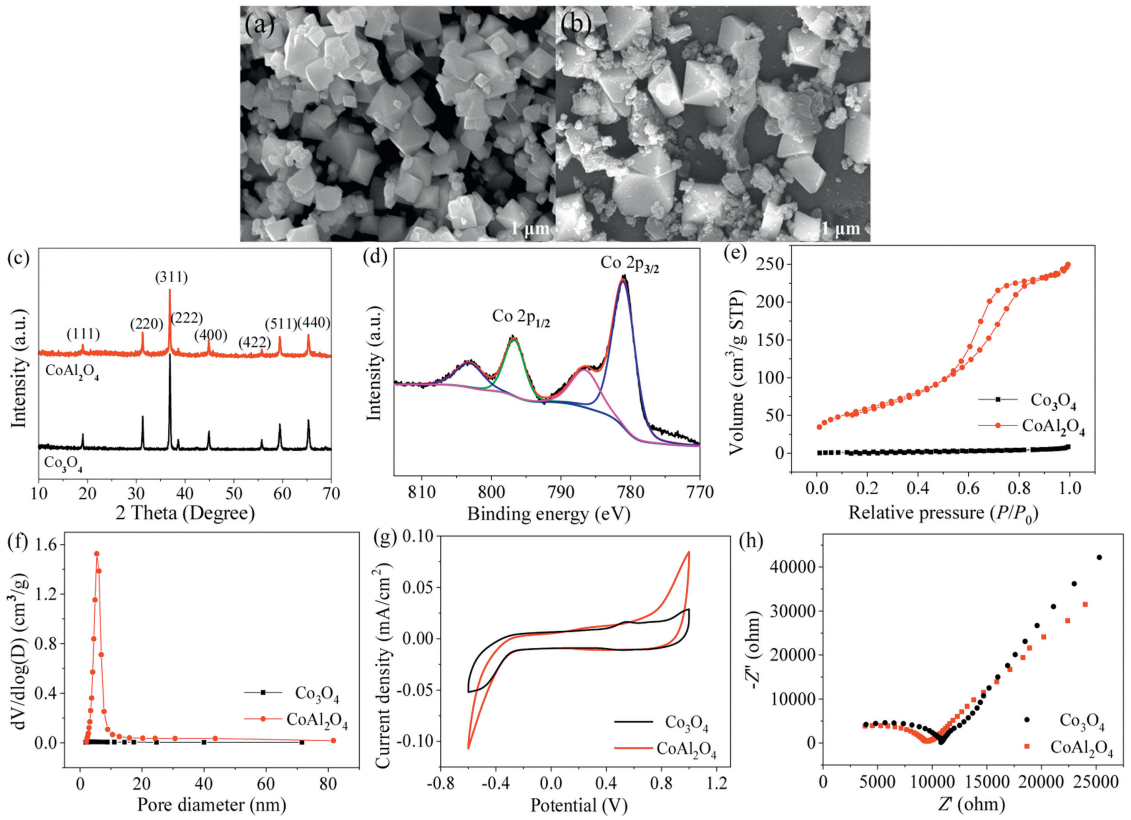

Fig. 1. SEM images of (a) Co_3O_4 and (b) $CoAl_2O_4$, (c) XRD patterns of Co_3O_4 and $CoAl_2O_4$, (d) Co 2p XPS spectrum of $CoAl_2O_4$, (e) N_2 adsorption-desorption isotherm curves, (f) pore size distributions, CV (g) and EIS Nyquist (h) plots of Co_3O_4 and $CoAl_2O_4$.

X-ray photoelectron spectroscopy (XPS) was performed to verify the formation of pure $CoAl_2O_4$. As displayed in Fig. 1d, the high-resolution spectrum of Co 2p is deconvoluted into two peaks centered at 781.0 and 796.7 eV, which correspond to Co $2p_{3/2}$ and Co $2p_{1/2}$, respectively. Satellite peaks are also visible at around 786.5 and 803.1 eV [26]. The energy separation between the spin-orbit doublets is 15.7 eV, which is characteristic of Co^{2+}. Moreover, no peak can be observed in the vicinity of 780 eV, thereby indicating the absence of the Co_3O_4 phase [25].

As shown in Fig. 1e, the N_2 sorption isotherm of $CoAl_2O_4$ corresponds to a typical IV isotherm with a H3 hysteresis loop, which indicates the presence of mesopores in $CoAl_2O_4$ [27]. In contrast, no hysteresis loop can be observed in the N_2 sorption isotherm of Co_3O_4, which indicates a non-mesoporous structure. These results can be further confirmed by the Barrett-Joyner-Halenda (BJH) pore diameter distribution, as demonstrated in Fig. 1f. Moreover, the specific surface area of $CoAl_2O_4$ (216.2 m^2/g) is 28 times higher than that of Co_3O_4 (7.7 m^2/g). Thus, $CoAl_2O_4$ was expected to provide more active sites that facilitate adsorption and reaction processes.

Electrochemical tests were conducted to evaluate the charge transfer capacities of Co_3O_4 and $CoAl_2O_4$. As shown in Fig. 1g, the cyclic voltammetry (CV) curve of $CoAl_2O_4$ exhibits a larger loop area than that of Co_3O_4, indicating a superior electron transfer capability. Meanwhile, the electrochemical impedance spectroscopy (EIS) Nyquist plots of $CoAl_2O_4$ correspond to a smaller charge transfer resistance than that of Co_3O_4 (Fig. 1h), suggesting a more efficient electron transfer in $CoAl_2O_4$.

The catalytic activities of the as-obtained catalysts were assessed by the oxidative degradation of RhB through PMS activation. As shown in Fig. 2a, in 40 min, $CoAl_2O_4$ adsorbed a negligible amount of RhB, and only 4.3% of RhB was degraded by PMS. In the presence of PMS, 18.1% of RhB was degraded by Co_3O_4 after 40 min, while $CoAl_2O_4$ degraded 99.5% of RhB, which was significantly higher than $CoAl_2O_4$-p (53.5%). Meanwhile, the degradation rate constant (fitted by applying *pseudo*-first-order kinetics) of RhB by $CoAl_2O_4$/PMS (0.178 min^{-1}) was calculated to be 89.0 and 10.5 times higher than those of $CoAl_2O_4$-p/PMS (0.017 min^{-1}) and Co_3O_4/PMS (0.002 min^{-1}), respectively. The superior catalytic performance of $CoAl_2O_4$ can be attributed to its large surface area, mesoporous structure, and decent electron transfer capability. Moreover, $CoAl_2O_4$ exhibited a better catalytic performance for PMS activation than many other spinel-type oxides (Table 1) [20–22, 28–31].

To explore the effect of $CoAl_2O_4$ dosage, PMS concentration, and solution pH on the reaction rate, a series of experiments were performed to obtain the optimal reaction conditions. As shown in Fig. 2b, the increase of the $CoAl_2O_4$ dosage provided more active sites, which led to the rapid degradation of RhB [32]. The increase of the PMS concentration from 0.05 g/L to 0.10 g/L also accelerated the degradation of RhB (Fig. 2c), while the continued increase of the PMS concentration up to 0.15 g/L did not significantly impact the degradation rate due to the self-quenching of generated reactive species [33]. In general, PMS based AOPs are highly dependent on the solution pH. In this work, the optimal pH value was determined to be between 5.0 and 7.0, in which 99.0% of RhB was degraded within 20 min (Fig. 2d). At a low pH of 3.0, H_2SO_5 would be the predominant species instead of HSO_5^- [34]. At a high pH of 9.0, the excess OH^- ions would scavenge $SO_4^{\bullet-}$, leading to a low RhB degradation efficiency [35].

Anions, such as Cl^-, HCO_3^-, and CO_3^{2-}, are ubiquitous in most wastewater. Therefore, their effects on the degradation of RhB in the $CoAl_2O_4$/PMS system were evaluated from a practical point of view. As shown in Fig. 3a, the RhB degradation rate of the system increased in the presence of Cl^-. According to existing literature, Cl^- may directly react with PMS to generate HClO that can promote the degradation of pollutants [36,37]. HCO_3^- and CO_3^{2-} are generally employed as radical scavengers in AOPs. Thus, they were expected to demonstrate an inhibiting effect on the degradation of RhB [38]. Moreover, HCO_3^- and CO_3^{2-} contributed to the increase of the solution pH, which also suppressed RhB degradation, as confirmed by the aforementioned pH study. The catalytic performance of $CoAl_2O_4$ for activating PMS to degrade typical dyes (cationic dye-MB, anionic dye-MO) and antibiotics (TCH) was examined. As illustrated in Fig. 3b, more than 90.0% of these pollutants were degraded, thereby establishing the general applicability of $CoAl_2O_4$.

The reusability and stability of catalysts are crucial in practical applications. As shown in Fig. 3c, $CoAl_2O_4$ demonstrated excellent catalytic performance in each cycle, and more than 94.0% of RhB was degraded by the sixth run. The minor deactivation of the catalyst can be attributed to the surface of $CoAl_2O_4$ being corroded during the reaction [39]. The concentration of the leached cobalt ions in the $CoAl_2O_4$/PMS system was determined to be 0.41 mg/L, which is lower than that in the Co_3O_4/PMS system (0.56 mg/L) and is below the concentration limit of cobalt ions (1 mg/L) according to the Environmental Quality Standard of Surface Water (GB3838-2002) issued in China. After RhB degradation, the main characteristic XRD peaks of $CoAl_2O_4$ remained unchanged (Fig. 3d). The results reveal the excellent reusability and stability of $CoAl_2O_4$ for PMS activation to degrade aqueous organic pollutants.

The existence of different ROS and their contributions to RhB degradation were further explored by radical quenching experiments and electron paramagnetic resonance (EPR) tests. As demonstrated in Fig. 3e, when 0.1 mol/L of *tert*-butyl alcohol (TBA) was introduced to the reaction solution, the degradation of RhB was slightly inhibited and the degradation rate decreased from 0.178 min^{-1} to 0.102 min^{-1}. In contrast, an addition of 0.1 mol/L of ethanol (EtOH) remarkably reduced the degradation rate to 0.026 in^{-1}. These results establish that $SO_4^{\bullet-}$ worked as the predominant ROS during the activation of PMS by $CoAl_2O_4$. EPR

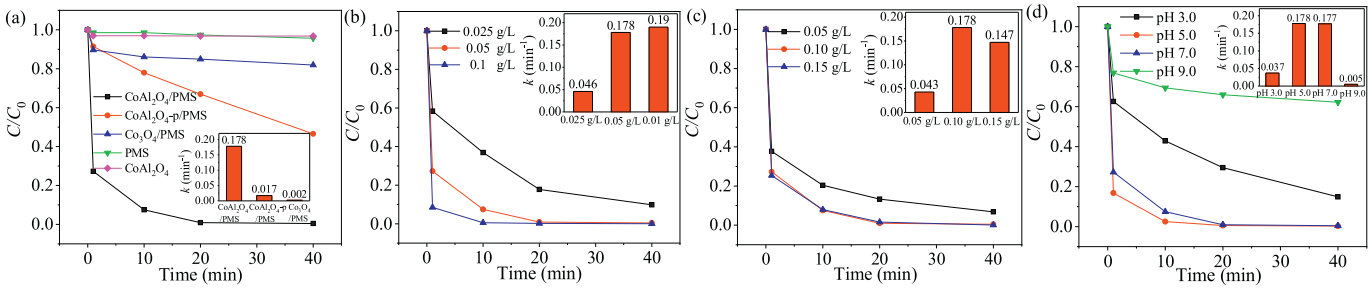

Fig. 2. (a) Degradation of RhB by different systems, effects of (b) $CoAl_2O_4$ dosage, (c) PMS concentration, and (d) solution pH on the degradation of RhB in the $CoAl_2O_4$/PMS system.

Table 1
Comparison of $CoAl_2O_4$ with other spinel-type catalysts in references.

Catalyst dosage (g/L)	PMS dosage (mmol/L)	Pollutant concentration and volume (mg/L*mL)	Removal efficiency	Reference
$CoFe_2O_4$ (0.4)	0.8	atrazine 10*100	99% (30 min)	[20]
$CuCo_2O_4$ (0.1)	0.65	benzophenone-4 10*200	99% (30 min)	[21]
$NiCo_2O_4$ (0.2)	0.5	humic acid 10*50	93% (60 min)	[22]
$MnFe_2O_4$ (0.2)	0.1	RhB 5*100	98% (30 min)	[28]
$CuBi_2O_4$ (0.8)	0.65	RhB 25*250	92% (90 min)	[29]
$NiCo_2O_4$ (0.2)	0.5	RhB 25*60	99% (40 min)	[30]
$CoFe_2O_4$ (0.5)	0.8	RhB 20*60	66% (40 min)	[31]
$CoAl_2O_4$ (0.1)	0.15	RhB 10*200	99% (20 min)	This work

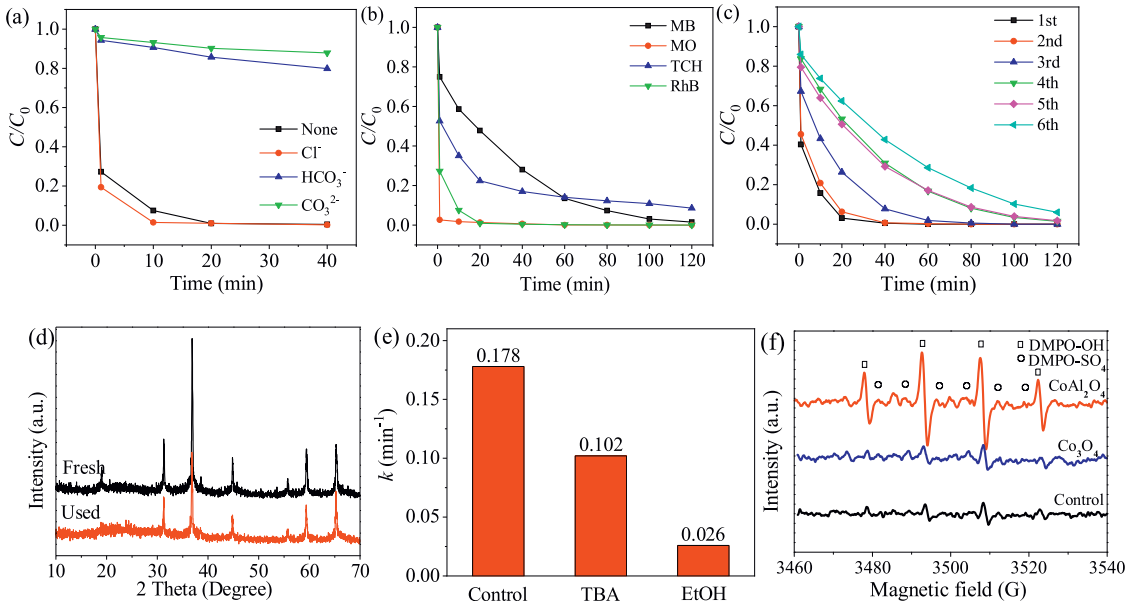

Fig. 3. (a) Effect of anions on the degradation of RhB in the $CoAl_2O_4$/PMS system. (b) Degradation of different contaminants in the $CoAl_2O_4$/PMS system. (c) Recycling experiments for RhB degradation in the $CoAl_2O_4$/PMS system. (d) XRD patterns of $CoAl_2O_4$ before and after the reaction. (e) Comparison of reaction rates under different quenching conditions, and (f) EPR spectra of DMPO-$^{\bullet}$OH and DMPO-$SO_4^{\bullet-}$ adducts in different systems.

measurements utilizing DMPO as a spin-trapping agent were conducted to verify the generation of $SO_4^{\bullet-}$ and $^{\bullet}$OH. As illustrated in Fig. 3f, the signals of DMPO-$^{\bullet}$OH and DMPO-$SO_4^{\bullet-}$ can be observed. Moreover, the intensity of such signals from $CoAl_2O_4$ was much higher than that of Co_3O_4, indicating that a larger number of $SO_4^{\bullet-}$ and $^{\bullet}$OH were generated in the $CoAl_2O_4$/PMS system [40].

In summary, a mesoporous $CoAl_2O_4$ spinel that is highly efficient for the degradation of RhB, MB, MO, and TCH was prepared through a combustion approach. The as-obtained $CoAl_2O_4$ was discovered to be extremely efficient in activating PMS, as evident from its RhB degradation rate of 0.178 min^{-1}, which is significantly higher than those of $CoAl_2O_4$-p (0.017 min^{-1}), Co_3O_4 (0.002 min^{-1}), and many other spinel-type catalysts used for pollutant degradation. The presence of HCO_3^- and CO_3^{2-} significantly suppressed the degradation of RhB, whereas the addition of Cl^- slightly promoted it. Radical quenching experiments and EPR tests revealed that both $SO_4^{\bullet-}$ and $^{\bullet}$OH were present in the $CoAl_2O_4$/PMS system, and $SO_4^{\bullet-}$ was the dominant ROS. The excellent catalytic performance of the $CoAl_2O_4$ spinel can be ascribed to its large surface area, mesoporous structure, and good electrical conductivity, which facilitate the generation of ROS for RhB removal. The excellent reusability and adaptability of the $CoAl_2O_4$ spinel render it a suitable candidate for pollutant degradation in PMS-based AOPs.

Declaration of competing interest

The authors declare that they have no known competing financial interests or personal relationships that could have appeared to influence the work reported in this paper.

Acknowledgments

This work received financial support from the National Natural Science Foundation of China (No. 51604194), China Scholarship Council (No. 201808420137), and Nanyang Environment and Water Research Institute (Core Fund), Nanyang Technological University, Singapore.

Appendix A. Supplementary data

Supplementary material related to this article can be found, in the online version, at doi:https://doi.org/10.1016/j.cclet.2021.01.019.

References

[1] J. Liu, X.C. Zhang, Q. Zhong, et al., J. Mater. Chem. A 8 (2020) 4083–4090.
[2] Y.D. Guo, C.X. Li, Z.H. Gong, et al., J. Hazard. Mater. 397 (2020) 122580.
[3] Q.K. Chen, L. Chen, J.J. Qi, et al., Chin. Chem. Lett. 30 (2019) 1214–1218.
[4] Z.P. Wen, J. Lu, Y.L. Zhang, et al., Chem. Eng. J. 391 (2020) 123578.

[5] S. Guo, W. Yang, L.M. You, et al., Chem. Eng. J. 393 (2020) 124758.
[6] S. Guo, G.K. Zhang, J.Q. Wang, J. Colloid Interface Sci. 433 (2014) 1–8.
[7] M.M. Du, Q.Y. Yi, J.H. Ji, et al., Chin. Chem. Lett. 31 (2020) 2803–2808.
[8] A. Jawad, K. Zhan, H.B. Wang, et al., Environ. Sci. Technol. 54 (2020) 2476–2488.
[9] C. Li, W. Yang, S. Guo, et al., Funct. Mater. Lett. 12 (2019) 1950083.
[10] X.Y. Wu, W.H. Zhao, Y.H. Huang, G.K. Zhang, Chem. Eng. J. 381 (2020) 122768.
[11] H. Tang, Z. Dai, X.D. Xie, Z.P. Wen, R. Chen, Chem. Eng. J. 356 (2019) 472–482.
[12] F. Rehman, M. Sayed, J.A. Khan, et al., J. Hazard. Mater. 337 (2018) 506–514.
[13] X.G. Duan, H.Q. Sun, J. Kang, et al., ACS Catal. 5 (2015) 4629–4636.
[14] S. Guo, Z.X. Yang, H.L. Zhang, et al., J. Mater. Sci. Technol. 62 (2021) 34–43.
[15] J.L. Zhu, J. Wang, C. Shan, et al., Chem. Eng. J. 375 (2019) 122009.
[16] Q. Zhao, Z.H. Yan, C.C. Chen, J. Chen, Chem. Rev. 117 (2017) 10121–10211.
[17] T. Wu, S. Sun, J. Song, et al., Nat. Catal. 2 (2019) 763–772.
[18] S. Khademolhoseini, R. Talebi, J. Mater. Sci. Mater. El. 27 (2016) 2938–2943.
[19] T. Gholami, M. Salavati-Niasari, S. Varshoy, Int. J. Hydrogen Energy 41 (2016) 9418–9426.
[20] J. Li, M.J. Xu, G. Yao, B. Lai, Chem. Eng. J. 348 (2018) 1012–1024.
[21] Y.P. Wang, H.D. Ji, W. Liu, et al., ACS Appl. Mater. Interfaces 12 (2020) 20522–20535.
[22] X.K. Tian, C. Tian, Y.L. Nie, et al., Chem. Eng. J. 331 (2018) 144–151.
[23] W. Li, J. Li, J. Guo, J. Eur. Ceram. Soc. 23 (2003) 2289–2295.
[24] A.J. Reynoso, U. Iriarte-Velasco, M.A. Gutiérrez-Ortiz, J.L. Ayastuy, Catal. Today 367 (2021) 278-289.
[25] C. MÁlvarez-Docio, J.J. Reinosa, A.D. Campo, J.F. Fernandez, J. Alloys Compd. 779 (2019) 244–254.
[26] X.L. Duan, M. Pan, F.P. Yu, D.R. Yuan, J. Alloys Compd. 509 (2011) 1079–1083.
[27] J.B. Xi, Q.J. Wang, J. Liu, et al., J. Catal. 359 (2018) 233–241.
[28] J. Deng, M.Y. Xu, C.G. Qiu, et al., Appl. Surf. Sci. 459 (2018) 138–147.
[29] Y.P. Wang, F. Li, T.S. Xue, et al., Environ. Sci. Pollut. Res. 25 (2018) 4419–4434.
[30] W.Y. Zhang, Y. Su, X.M. Zhang, Y. Yang, X.H. Guo, RSC Adv. 6 (2016) 64626–64633.
[31] P. Niu, C.H. Li, C.X. Jia, D.Q. Wang, S.W. Liu, J. Sol-Gel Sci. Technol. 93 (2020) 419–427.
[32] Y. Liu, H.G. Guo, Y.L. Zhang, et al., Chem. Eng. J. 356 (2019) 717–726.
[33] P.D. Hu, M.C. Long, X. Bai, et al., J. Hazard. Mater. 332 (2017) 195–204.
[34] S. Guo, H.J. Wang, W. Yang, et al., Appl. Catal. B: Environ. 262 (2020) 118250.
[35] N. Tian, X.K. Tian, Y.L. Nie, et al., Chem. Eng. J. 355 (2019) 448–456.
[36] Y.B. Wang, D. Cao, X. Zhao, Chem. Eng. J. 328 (2017) 1112–1121.
[37] R. Luo, M. Li, C. Wang, et al., Water Res. 148 (2019) 416–424.
[38] W. Ren, P. Zhou, G. Nie, et al., Water Res. 186 (2020) 116361.
[39] Y. Feng, D.L. Wu, Y. Deng, T. Zhang, K. Shih, Environ. Sci. Technol. 50 (2016) 3119–3127.
[40] Y. Zhao, H.Z. An, J. Feng, Y.M. Ren, J. Ma, Environ. Sci. Technol. 53 (2019) 4500–4510.